

Detection of the BL Lac Object 1H1426+428 at TeV Gamma Ray Energies

D. Horan,^{1,2} H. M. Badran,^{1,7} I. H. Bond,³ S. M. Bradbury,³ J. H. Buckley,⁴ M. J. Carson,² D. A. Carter-Lewis,⁵ M. Catanese,¹ W. Cui,¹⁰ S. Dunlea,² D. Das,¹⁵ I. de la Calle Perez,³ M. D'Vali,³ D. J. Fegan,² S. J. Fegan,^{1,8} J. P. Finley,⁶ J. A. Gaidos,⁶ K. Gibbs,¹ G. H. Gillanders,⁹ T. A. Hall,^{5,17} A. M. Hillas,³ J. Holder,³ M. Jordan,⁴ M. Kertzman,¹⁶ D. Kieda,¹¹ J. Kildea,² J. Knapp,³ K. Kosack,⁴ F. Krennrich,⁵ M. J. Lang,⁹ S. LeBohec,⁵ R. Lessard,⁶ J. Lloyd-Evans,³ B. McKernan,² P. Moriarty,¹³ D. Muller,¹⁰ R. Ong,¹² R. Pallassini,³ D. Petry,⁵ J. Quinn,² N. W. Reay,¹⁵ P. T. Reynolds,¹⁴ H. J. Rose,³ G. H. Sembroski,⁶ R. Sidwell,¹⁵ N. Stanton,¹⁵ S. P. Swordy,¹⁰ V. V. Vassiliev,¹¹ S. P. Wakely,¹⁰ T. C. Weekes¹

dhoran@cfa.harvard.edu

ABSTRACT

¹Fred Lawrence Whipple Observatory, Harvard-Smithsonian CfA, P.O. Box 97, Amado, AZ 85645

²Experimental Physics Department, National University of Ireland, Belfield, Dublin 4, Ireland

³Department of Physics, University of Leeds, Leeds, LS2 9JT, Yorkshire, England, UK

⁴Department of Physics, Washington University, St. Louis, MO 63130

⁵Department of Physics and Astronomy, Iowa State University, Ames, IA 50011

⁶Department of Physics, Purdue University, West Lafayette, IN 47907

⁷Physics Department, Tanta University, Tanta, Egypt

⁸Department of Physics, University of Arizona, Tucson, AZ 85721

⁹Physics Department, National University of Ireland, Galway, Ireland

¹⁰Enrico Fermi Institute, University of Chicago, Chicago, IL 60637

¹¹High Energy Astrophysics Institute, University of Utah, Salt Lake City, UT 84112

¹²Department of Physics, University of California, Los Angeles, CA 90095

¹³School of Science, Galway-Mayo Institute of Technology, Galway, Ireland

¹⁴Department of Physics, Cork Institute of Technology, Cork, Ireland

¹⁵Department of Physics, Kansas State University, Manhattan, KS 66506

¹⁶Department of Physics and Astronomy, DePauw University, Greencastle, IN 46135

¹⁷Physics & Astronomy Department, University of Arkansas at Little Rock, Little Rock, AR 72204

A very high energy γ -ray signal has been detected at the 5.5σ level from 1H1426+428, an x-ray selected BL Lacertae object at a redshift of 0.129. The object was monitored from 1995 - 1998 with the Whipple 10m imaging atmospheric Čerenkov telescope as part of a general blazar survey; the results of these observations, although not statistically significant, were consistently positive. X-ray observations of 1H1426+428 during 1999 with the *BeppoSAX* instrument revealed that the peak of its synchrotron spectrum occurs at > 100 keV, leading to the prediction of observable TeV emission from this object. 1H1426+428 was monitored extensively at the Whipple Observatory during the 1999, 2000, and 2001 observing seasons. The strongest TeV signals were detected in 2000 and 2001. During 2001, an integral flux of $2.04 \pm 0.35 \times 10^{-11}$ cm $^{-2}$ s $^{-1}$ above 280 GeV was recorded from 1H1426+428. The detection of 1H1426+428 supports the idea that, as also seen in Markarian 501 and 1ES2344+514, BL Lacertae objects with extremely high synchrotron peak frequencies produce γ -rays in the TeV range.

Subject headings: BL Lacertae objects: individual (1ES 1426+42.8) — gamma rays: observations

1. Introduction

Blazars are the main class of Active Galactic Nuclei (AGN) detected above 100 MeV by the EGRET experiment on the Compton Gamma Ray Observatory (CGRO) and by ground-based γ -ray observatories (Mukherjee et al. 1997; Weekes 2001). They comprise a subclass of AGN and are characterized by a highly variable non-thermal continuum, strong variable optical polarization, the lack of a UV-excess (or “blue bump”) and a core-dominated radio morphology. BL Lacertae (BL Lac) objects are a subclass of blazars that are notable for their lack of prominent emission lines. The broad-band double-humped Spectral Energy Distributions (SEDs) of BL Lacs identified in x-ray surveys differ significantly from the SEDs of those identified in radio surveys. This led to the sub-classification of BL Lacs into High-frequency-peaked BL Lacs (HBLs) and Low-frequency-peaked BL Lacs (LBLs) based on the ratio of their x-ray to radio flux densities (Padovani & Giommi 1995). The first “hump”, generally assumed to be the peak of the synchrotron emission (in a νF_ν representation), is in the IR-optical for LBLs and in the EUV-soft x-ray band for HBLs. BL Lac objects make up a significant fraction of the 70 blazars in the 3rd EGRET Catalog (Hartman et al. 1999) and most of them are classified as LBLs. It has been shown that there is not a sharp division between these two classes of objects (see, e.g., Fossati et al. 1998; Ghisellini 1999).

Recent studies with ground-based γ -ray telescopes have produced evidence for TeV γ -ray emission from seven BL Lac objects, five of which are classified as HBL and two as LBL (Weekes 2001). The most prominent of these are Markarian 421 (Mrk 421), which has been detected by five ground based imaging atmospheric Čerenkov γ -ray observatories, and Markarian 501 (Mrk 501), which has been detected by six such observatories. The emission from both of these objects can be explained by Compton-synchrotron models although detailed modeling is still fraught with many uncertainties. Both objects are characterized by rapid variability on time-scales from hours to months. In the TeV energy range, the energy spectrum of Mrk 501 and, more recently, that of Mrk 421, have been shown to exhibit absorption-like features (Krennrich et al. 1999; Aharonian et al. 1999; Krennrich et al. 2001). The temporal and spectral properties of the other TeV BL Lacs are less well defined.

Since 1992, the Whipple Gamma Ray collaboration, using the 10m imaging atmospheric Čerenkov telescope on Mt. Hopkins, has been searching for TeV γ -ray emission from AGN. Initially the search was concentrated on blazars detected by EGRET at any redshift; these observations led to the detection of Mrk 421 (Punch et al. 1992) and upper limits on some 30 other blazars (Kerrick et al. 1995). More recently, the search has concentrated on nearby BL Lacs leading to the detection of Mrk 501 (Quinn et al. 1996) and 1ES 2344+514 (Catanese et al. 1998). Between 1995 and 1998, the survey included 24 objects (17 HBLs, 7 LBLs) ranging in redshift from 0.046 to 0.44; the results for these objects will be published shortly (D. Horan et al., in preparation). Although none of these observations resulted in a detection, the observations of 1H1426+428 yielded the highest consistently positive statistical significances.

In this paper, evidence is presented for the detection of very high energy (VHE) γ -rays from 1H1426+428. The 1H1426+428 observations are divided into two categories - those taken as part of the general blazar survey between 1995 and 1998, and the subsequent concentrated observations carried out between 1999 and 2001. A preliminary energy spectrum is derived and the implications of the detection of 1H1426+428 at these energies are discussed.

2. 1H1426+428 at Other Wavelengths

1H1426+428 was discovered in the 2-6 keV band by HEAO-1 (Wood et al. 1984) and was classified as a BL Lac object in 1989 (Remillard et al. 1989). It has a cosmological redshift of 0.129 and is located in the constellation of Boötes ($\alpha_{J2000} = 14^h 28^m 32^s.7$, $\delta_{J2000} = +42^\circ 40' 20''$). It is an optically faint object ($m_V = 16.9$) and is believed to be at the center of an elliptical galaxy. 1H1426+428 is bright in the x-ray band with a 2-6 keV luminosity of $\sim 10^{44}$ erg s $^{-1}$ which is typical of the BL Lacs found with HEAO-1. Both the flux of 1H1426+428 in the 2-10 keV band and its spectral index above 2 keV have been found to

change over time (Costamante et al. 2001).

Three recent BL Lac surveys, DXRBS (Perlman et al. 1998), RGB (Laurent-Muehleisen et al. 1999), and REX (Caccianiga et al. 1999), have shown that, despite the conventional subdivision into HBLs and LBLs, BL Lacs actually form a continuous class with respect to the peak of the synchrotron emission, which smoothly ranges between IR and soft x-ray frequencies and up to the 2-10 keV band for sources like Mrk 421. *Beppo-SAX* observations of Mrk 501 (Pian et al. 1998) and 1ES 2344+514 (Giommi, Padovani, & Perlman 2000) revealed that, at least in a flaring state, the first peak of the SED can reach even higher energies, at or above 100 keV.

In 1998-1999, *Beppo-SAX* performed an observing campaign with the aim of finding and studying other sources as “extreme” as Mrk 501 is in its flaring state. The candidates for the *Beppo-SAX* survey were selected from the Einstein Slew Survey and the RASSBSC catalogs. These *Beppo-SAX* observations (Costamante et al. 2000a, 2000b, 2001) revealed four new “extreme” HBLs, selected because they have high synchrotron peak frequencies and are therefore possible TeV emitters. These four candidates for TeV emission were: 1ES 0120+340, PKS 0548-322, 1ES 1426+42.8 (i.e. 1H1426+428) and H2356-309.

The spectra for three of these objects (1ES 0120+340, PKS 0548-322, and H2356-309) were well fitted by a convex broken power law with a break energy, and hence the peak of the synchrotron emission, occurring at about 1.4 keV for 1ES0120+340, 4.4 keV for PKS0548-322 and 1.8 keV for H2356-309. In the case of 1H1426+428 however, no evidence for a spectral break up to 100 keV was found. Instead, its spectrum was well fitted by a single power-law, with a flat spectral index of 0.92 up to 100 keV, thus constraining the peak of the synchrotron emission to lie near or above this value. The best fit of a pure homogeneous synchrotron self-Compton (SSC) model for 1H1426+428 (Costamante et al. 2000a) predicted detectable γ -ray emission at TeV energies. At the time of the *Beppo-SAX* observation the observed x-ray flux in the 2-10 keV band was at one of the lowest levels ever recorded from 1H1426+428, indicating that it was not in a flaring state (Costamante et al. 2001). This implies that, in the event of a flare, the synchrotron peak could shift to even higher values as was observed for both Mrk 501 and 1ES 2344+514. It also indicates that highly relativistic electrons are present which makes 1H1426+428 the most promising candidate for TeV emission from this survey.

3. Observing Technique

The observations reported in this paper were taken with the 10m reflector at the Whipple Observatory on Mount Hopkins in southern Arizona (elevation 2.3 km) using the atmospheric Čerenkov imaging technique. During the course of the observations presented here, many changes were implemented on the 10m telescope. The imaging camera (Cawley et al. 1990) was upgraded a number of times (Finley et al. 2000), the number of photo-multiplier tubes (PMTs) being increased with each iteration, resulting in the current high resolution, 490 pixel camera (Finley et al. 2001). The triggering electronics were upgraded to a Pattern Selection Trigger (Bradbury et al. 1999) and light cones were installed in front of the PMTs to increase their light collection efficiency. The unprotected, anodized, front-aluminized mirrors on the 10m were recoated during the timespan of the observations. Because of changes in PMT configuration, triggering, mirror reflectivity, and light collection efficiency, the energy response of the camera for γ -ray detection varied. Since various changes were made at the beginning of each observing season (typically between June and September), it is convenient to consider each observing season separately and to characterize it by the observed response from the assumed standard candle, the Crab Nebula. The different configurations of the camera and the resultant peak response energies are summarized in Table 1.

Table 1. Camera configurations from 1995 - 2001.

Period	No. of Pixels	Spacing ($^{\circ}$)	FOV ^a ($^{\circ}$)	Light Cones	Trigger	E_{peak}^b (GeV)
1995/01 - 1996/12	109	0.259	3.0	yes	majority	300
1997/01 - 1997/06	151	0.259	3.3	yes	majority	350
1997/09 - 1998/12	331	0.24	4.8	no	majority	500
1999/03 - 1999/06	331	0.24	4.8	yes	pattern	500
1999/09 - 2000/07	490	0.12 ^c	3.8 ^d	yes	pattern	430
2000/10 - 2001/06	490	0.12 ^c	3.8 ^d	yes	pattern	390

^aField of view (FOV).

^bThe peak response energy (E_{peak}); this is the energy at which the collection area folded with an $E^{-2.5}$ spectrum reaches a maximum. Thus, it is the energy at which the camera is most efficient at detecting γ -rays. These values are subject to a $\sim 20\%$ uncertainty. Although E_{peak} has increased somewhat over time, this does not mean that the camera is now poorer at detecting the lower energy γ -rays. In fact, the collection area of the telescope at 300 GeV in the 1999 - 2000 observing season, was greater than the collection area at this energy in the 1995 - 1996 observing season.

^cThe spacing between the outer tubes is 0.24° .

^dThe outer rings of tubes were not used in this analysis, hence the field of view here is effectively 2.6° .

The Čerenkov light images from each shower are analyzed off-line using a moment analysis (Reynolds et al. 1993). The derived image parameters are used to distinguish candidate γ -rays from the large background of cosmic-rays. These parameters include *length*, *width*, *distance* (from the optic axis), and orientation (*alpha*). In addition, the two highest recorded signals in individual pixels (*sig1* and *sig2*) are noted as well as the total light in the image (*size*). Monte Carlo simulations were used to determine the approximate limits on the parameters to be used for the identification of candidate γ -ray images; these limits were then optimized on contemporaneous observations of the Crab Nebula. The results of an analysis are graphically presented as a histogram of the *alpha* parameter - usually referred to as an alpha plot. In such histograms, the *alpha* values for all the events that passed all γ -ray selection criteria except for the *alpha* cut, are plotted. For a γ -ray source, an excess would be expected at low values of *alpha*.

Two modes of observation were used: ON/OFF and TRACKING. In ON/OFF mode, a 28 sidereal minute run is taken with the candidate γ -ray source at the center of the field of view - the ON run. The OFF run, a 'control' run, is also taken for 28 sidereal minutes through the same range of azimuth and elevation, thus enabling this region of the atmosphere to be characterised in the absence of the γ -ray candidate. In the TRACKING mode, the object is continuously tracked for 28 sidereal minutes with no control run being taken.

Even in the absence of a γ -ray source, a certain percentage of events recorded will pass all of the γ -ray selection criteria. This background level of events, which depends on a number of factors including sky brightness, elevation, and weather, needs to be established in order to calculate the statistical significance of any apparent excess of γ -rays detected. There are different methods to estimate this background depending on which mode of observation was used.

For data taken in ON/OFF mode, the OFF scan provides an estimate of the number of γ -ray like events that would be recorded from this range of azimuth and elevation, in the absence of the candidate γ -ray source. In this data acquisition mode, differences in night-sky brightness between the ON and OFF regions of the sky can introduce a bias when the data are analyzed. In order to reduce this bias, the standard deviations of the night-sky background in each PMT are compared for the ON and the OFF runs. Gaussian noise is then added in quadrature to the signal from whichever region of the sky (ON or OFF) is the darker, so as to match the standard deviations for the tube in the ON and OFF runs. This technique is known as software padding and is described in Cawley (1993).

Unlike observations taken in the ON/OFF mode, scans taken in the TRACKING mode do not have independent control data. A background estimate is essential in order to predict what number of the background events, passing all cuts, would have been detected during the

scan in the absence of the candidate γ -ray source. Since most of the 1H1426+428 observations were taken in the TRACKING mode, two different methods of background estimation were used. Each of these methods is outlined below.

In the first method, which is the standard analysis method used for data taken in the TRACKING mode (Catanese et al. 1998), the alpha plot was characterized when there was no γ -ray source at the center of the field of view. This was done by analyzing 'darkfield data' which consisted of data taken in the OFF mode, and of observations of objects found not to be sources of γ -rays. A large database of these scans were analyzed, giving the shape that an alpha plot would be expected to have when no γ -rays are present.

Most γ -rays from an object at the center of the field of view will have small values of the *alpha* parameter. Hence, the *alpha* distribution beyond 20° can be assumed to be independent of the γ -ray source, and thus representative of the background level of γ -ray-like events in the field of view. Using the darkfield data, a ratio was calculated to scale the number of events between 20° and 65° to the number that pass the *alpha* cut. This ratio, the 'tracking ratio' (ρ), was then used to scale the 20° to 65° region of the alpha plot for the TRACKING scan, to estimate the background level of events passing all cuts. Its value and statistical uncertainty ($\Delta\rho$) are given by:

$$\rho \pm \Delta\rho = \frac{N_{\text{alpha}}}{N_{\text{control}}} \pm \sqrt{\frac{N_{\text{alpha}}}{N_{\text{control}}^2} + \frac{N_{\text{alpha}}^2}{N_{\text{control}}^3}} \quad (1)$$

where N_{alpha} is defined as the number of events in the darkfield data that pass all the γ -ray selection criteria including the *alpha* cut, while N_{control} is the number of such events with *alpha* between 20° and 65° . The tracking ratio was calculated using the darkfield data available for each observing year over the same range of elevation angles as the source observations. In addition, the tracking ratio was checked using the OFF data on 1H1426+428 from ON/OFF runs (where available); within statistics these tracking ratios were consistent with the standard tracking ratio derived from the full yearly database. To check for systematic effects associated with the determination of the global tracking ratio, the darkfield data were subdivided on the basis of the region of the sky which they were from. Each of these dark-sky regions was checked individually and the tracking ratio determined and compared to the global tracking ratio. It was found that the global tracking ratio and these individual tracking ratios were consistent within statistical uncertainty.

In the alternative method for estimating the background, each 1H1426+428 TRACKING scan was assigned a suitable OFF scan as its background. The OFF database comprised all OFF scans taken during the observing season including 1H1426+428 OFF runs. In order to establish the most suitable OFF scan for each 1H1426+428 TRACKING scan, each OFF run was

characterized by parameters pertinent to the conditions during the scan. These consisted of the elevation, the number of PMTs switched off and the mean night-sky background during that scan, along with the throughput factor recorded on the night of the scan and the date on which the scan was taken. The throughput factor (Holder et al. 2001) is a measure of sky clarity based on the spectrum of the total amount of light produced by background cosmic rays. The same information was assembled for each 1H1426+428 TRACKING scan. Then, for each 1H1426+428 TRACKING scan, the OFF scan whose conditions most closely matched it was deemed the most suitable background estimate, and was used as the background for that 1H1426+428 TRACKING run. In cases where there was not a suitable OFF run, the 1H1426+428 TRACKING run was omitted. With each 1H1426+428 TRACKING scan then having an associated OFF run, the data were analyzed as if they were taken in the ON/OFF mode, and hence, software padding was applied. The sky quality changes from night to night, causing variations of $\sim 10\%$ in the raw trigger rate, for data taken on the same source at the same elevation. Therefore, even after selecting OFF scans with run conditions which match those of the ON scans, it is still necessary to normalize the total number of events ON and OFF. We calculate the normalizing factor from the ratio of the number of events in the $30^\circ - 90^\circ$ control region of the ON and OFF alpha plots.

It was found that both methods of background estimation were consistent, and indicated excesses of similar significance, thus suggesting that the γ -ray excess can be reliably determined for TRACKING scans.

4. Database

For the purpose of data analysis, two different strategies were employed: (a) All of the data taken in the ON and the TRACKING modes were combined and subjected to a TRACKING analysis. (b) All of the data taken in the ON mode, along with their corresponding OFF data, were analyzed together using the PAIRS analysis. The γ -ray selection criteria, including the *alpha* bound, were re-optimized each year using data from the Crab Nebula. The optimum value for the *alpha* bound was found empirically to increase from 10° to 15° when the smaller, high resolution 490 pixel camera was installed in the summer of 1999.

4.1. 1995 - 1998 Observations

In June-July, 1995, 1H1426+428 was observed for 3.5 hours in the TRACKING mode with the 109 pixel camera (spacing 0.259° , 3.0° field of view and standard trigger). In February-

June, 1997, another 13.2 hours were used to observe 1H1426+428 in the TRACKING mode; the camera configuration was as before but the number of pixels was increased to 151. In April, 1998, 0.87 hours of 1H1426+428 data were taken; the 331 pixel camera was installed at this time with the standard trigger.

4.2. 1999 Observations

During the 1999 observing season, a total of 7 ON/OFF pairs and 51 TRACKING runs were taken with the 2-fold Pattern Selection Trigger. Three TRACKING runs were excluded from further analysis based on fluctuations in the raw rate and inferior weather conditions. This left a total of 24.35 hours (7 ON runs and 48 TRACKING runs) of data available for analysis. These observations were initiated as part of the general BL Lac survey (D. Horan et al., in preparation) with extra data being taken in 1999 because of an initial indication of a signal from 1H1426+428. A tracking ratio of 0.232 ± 0.005 was determined for $\alpha < 10^\circ$.

4.3. 2000 Observations

During the 2000 observing season, 33 ON/OFF pairs and 35 TRACKING runs were taken on 1H1426+428. Eleven ON source runs were excluded from further analysis based on fluctuations in the raw rate and inferior weather conditions, leaving a total of 26.46 hours of data available for TRACKING analysis (57 TRACKING/ON) and 13.86 hours of data in the ON/OFF mode (30 ON/OFF pairs). A tracking ratio of 0.312 ± 0.002 for $\alpha < 15^\circ$ was determined. 1H1426+428 OFF data were analyzed to ensure that this tracking ratio was consistent with the tracking ratio derived for these data.

4.4. 2001 Observations

A total of 42.24 hours were spent on the source during 2001; this comprised 39 ON/OFF pairs and 59 TRACKING runs. After excluding data taken at low elevation and in unsatisfactory weather conditions, 38.10 hours of data remained (34 ON/OFF pairs and 53 TRACKING runs). The tracking ratio for this observing season, again for $\alpha < 15^\circ$, was calculated to be 0.323 ± 0.002 . As with the 2000 data, checks were performed to ensure that this ratio was appropriate for the 1H1426+428 data. A summary of the data taken and analyzed in the 2000 and 2001 observing seasons is give in Table 2.

5. Results

5.1. 1995 - 1998 Observations

The observations of 1H1426+428 between 1995 and 1998 were analyzed as part of a general BL Lac survey. The results are summarized in Table 3. Although not statistically significant, 1H1426+428 was one of only two objects, out of the 24 objects observed in this survey, to show consistently positive results.

Table 2: Summary of the number of data scans taken and analyzed in 2000 and 2001.

Year	Data Recorded		Data Analyzed		
	TRACKING	ON	Standard	Alternative	PAIRS
2000	35 (27)	33 (30)	57	57	30
2001	59 (53)	39 (34)	87	71	34

Note. — The mode that the data were recorded in are given in the first two columns. The numbers in parentheses here refer to the number of usable data scans recorded. The final three columns give the number of scans analyzed in each of the three data analysis modes: standard TRACKING analysis, alternative TRACKING analysis or PAIRS.

Table 3. Summary of the Observations and Results for 1H1426+428 between 1995 and 1999.

Period	Exp. (hrs)	Total σ	Max. σ Month ^a	Max. σ Night ^b	Flux ^c ($\text{cm}^{-2} \text{ s}^{-1}$)
1995/06 - 1995/07	3.48	2.1	2.1	2.1	$<0.2 \times 10^{-11}$
1997/02 - 1997/06	13.16	1.7	2.2	1.6	$<0.1 \times 10^{-11}$
1998/04	0.87	1.7	1.7	2.0	$<6.7 \times 10^{-11}$
1999/03 - 1999/06	24.35	0.9	1.6	2.1	$<6.7 \times 10^{-11}$

^aThe maximum statistical significance of the signal recorded from 1H1426+428 when the data are grouped by the month during which they were recorded.

^bThe maximum statistical significance of the signal recorded from 1H1426+428 when the data are grouped by the night on which they were recorded.

^cThe integral fluxes are quoted at the peak response energy for the observation period, as given in Table 1.

5.2. 1999 Observations

A total of 24.35 hours of data were taken on 1H1426+428 during 1999. The net excess of $+0.9\sigma$ from the combined 1999 observations was not statistically significant.

5.3. 2000 Observations

A TRACKING analysis of all the on-source data taken on 1H1426+428 during 2000, using the standard tracking ratio calculated for that observing season, gave a $+4.2\sigma$ excess corresponding to a γ -ray rate of $0.24 \pm 0.06 \gamma \text{ min}^{-1}$. When these data were analyzed independently using the alternative method of background estimation, the excess was at the $+3.1\sigma$ level with a γ -ray rate of $0.21 \pm 0.07 \gamma \text{ min}^{-1}$. The alpha plot for these data is shown in Figure 1 (left panel) along with the alpha plot from the matched OFF data. The background shown on the figure (dashed line) consists of the OFF data which were chosen to match the characteristics of the 1H1426+428 TRACKING data. These data are scaled to match the 1H1426+428 data in the 30° - 90° region of the alpha plot. The net significance for the 30 ON/OFF pairs taken in 2000 was $+1.2\sigma$, with a γ -ray rate of $0.10 \pm 0.09 \gamma \text{ min}^{-1}$. The alpha plot for these data is shown in Figure 1 (right panel). On the night of May 30, 2000 (MJD 51694), the first TRACKING scan on 1H1426+428 gave a significance of $+3.0\sigma$, using the standard tracking ratio method of background estimation. This prompted observers to take four more TRACKING scans which led to the detection of a signal at the $+3.7\sigma$ for this night. The γ -ray rate for these 5 scans (2.15 hours) was $0.67 \pm 0.18 \gamma \text{ min}^{-1}$.

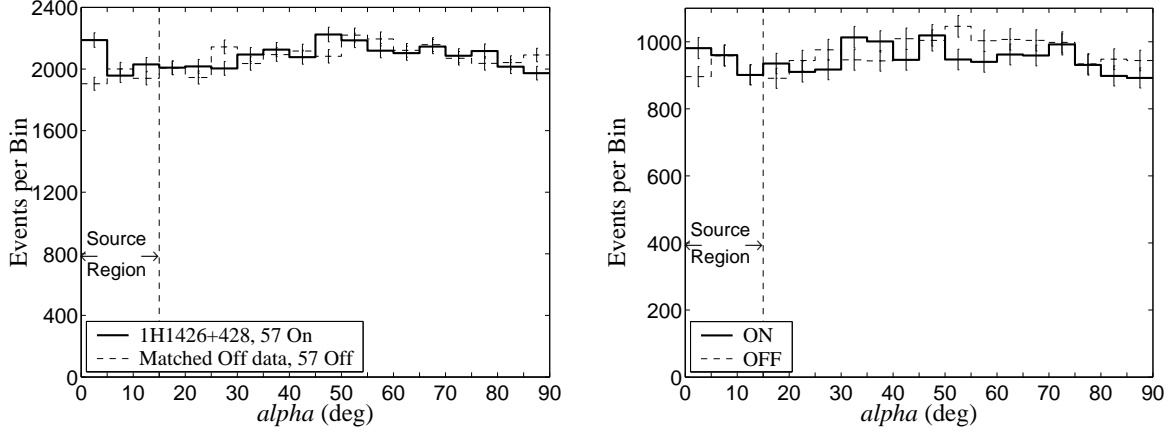


Fig. 1.— Left: Alpha plot for 26.49 hours of the data taken on 1H1426+428 during 2000. The total significance for these 57 scans is $+3.1\sigma$ when analyzed using the alternative method for estimating the background. The matched OFF data used to estimate the background level are also shown (dashed line). These are normalized to the 1H1426+428 data between α values of 30° and 90° . Right: Alpha plot for the 30 ON/OFF pairs taken in 2000. The net significance for these data is $+1.2\sigma$.

5.4. 2001 Observations

A TRACKING analysis of all of the on-source data taken on 1H1426+428 during 2001, using the tracking ratio calculated for this observing season, gave an excess of $+5.4\sigma$ corresponding to a γ -ray rate of $0.36 \pm 0.07 \gamma \text{ min}^{-1}$. An independent analysis of 31.13 hours of these data, using the alternative method of background estimation, resulted in a $+5.5\sigma$ excess with a γ -ray rate of $0.44 \pm 0.08 \gamma \text{ min}^{-1}$. The alpha plot for these data is shown in Figure 2 (left panel) along with the alpha plot from the matched OFF data. As before, these data are scaled to the 1H1426+428 data between *alpha* values of 30° and 90° .

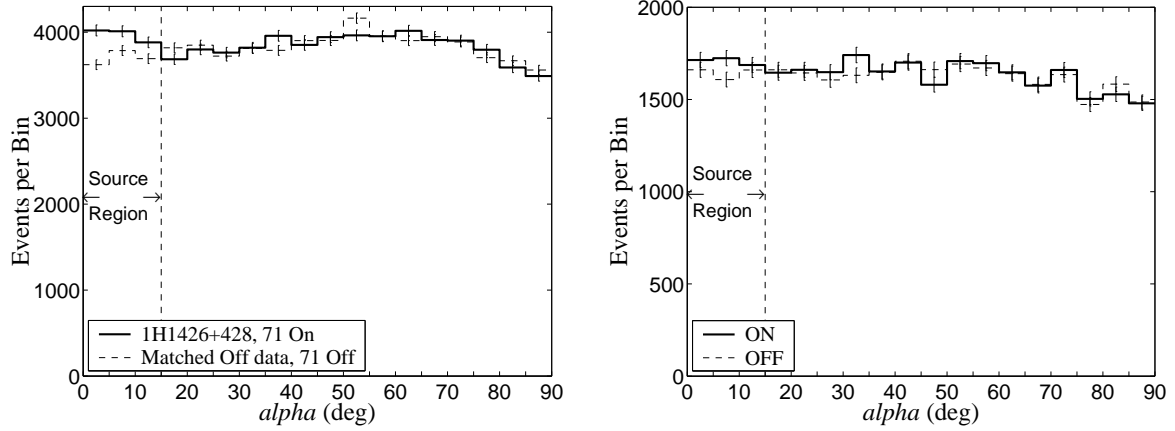


Fig. 2.— Left: Alpha plot for 31.13 hours of the data taken on 1H1426+428 during 2001. The total significance for these 71 scans, when analyzed using the alternative method of background estimation, is $+5.5\sigma$. The matched OFF data used to estimate the background level are also shown (dashed line). These are normalized to the 1H1426+428 data between α values of 30° and 90° . Right: Alpha plot for the 15.53 hours of data taken in the ON/OFF mode on 1H1426+428 during 2001. The total significance for these 34 ON/OFF pairs is $+2.0\sigma$.

The significance from the 34 ON/OFF pairs taken during the 2001 observing season is $+2.0\sigma$, with a γ -ray rate of $0.22 \pm 0.11 \gamma \text{ min}^{-1}$. The alpha plot for these data is shown in Figure 2 (right panel). A summary of the results of the observations made on 1H1426+428 during 2000 and 2001, using the alternative method of background estimation, is presented in Table 4.

Table 4. Summary of the results of 1H1426+428 observations during 2000 and 2001.

Period	Exp. (hrs)	Total σ	Max. σ	Month ^a
2000/02 - 2000/06	26.37	3.1	3.4	
2001/01 - 2001/06	31.12	5.5	5.0	

^aThe maximum statistical significance of the signal recorded from 1H1426+428 when the data are grouped by the month during which they were recorded.

When both the differences in exposure time and methods of background estimation are taken into account, the results from the ON/OFF pairs and the TRACKING data taken on 1H1426+428 during each observing season are consistent, at the 2σ level, with each other.

5.5. Comparison of the Gamma-Ray and X-Ray Flux from 1H1426+428

The γ -ray rates for the 2000 and 2001 1H1426+428 data were compared with the x-ray flux from the All Sky Monitor (ASM) instrument on board the Rossi X-ray Timing Explorer (RXTE; Levine et al. 1996). A correlation was sought between the nightly γ -ray rates and the “one-day average” x-ray data points. Only nights on which there were both x-ray and γ -ray data were considered when performing the correlation. This left 37 nights for analysis during 2000, and 39 nights during 2001.

Since γ -ray observations can only be taken on moonless nights, there are a few (~ 6) nights around the time of full moon each month, when no observations can be made. The periods during which the γ -ray data are taken are referred to as ‘darkruns’. Correlations between the x-ray and γ -ray rates were sought both over the entire observing season, and during darkruns with more than two nights on which both x-ray and γ -ray data were taken. No evidence for significant nightly correlation was found for either observing season. The x-ray and γ -ray rate curves are shown in Figure 3. The rates plotted here are the average monthly rates for the 2000 and 2001 data. The γ -ray rates shown were calculated using the alternative method of background estimation. There is some evidence for an anti-correlation between these average monthly rates, especially in the 2001 data.

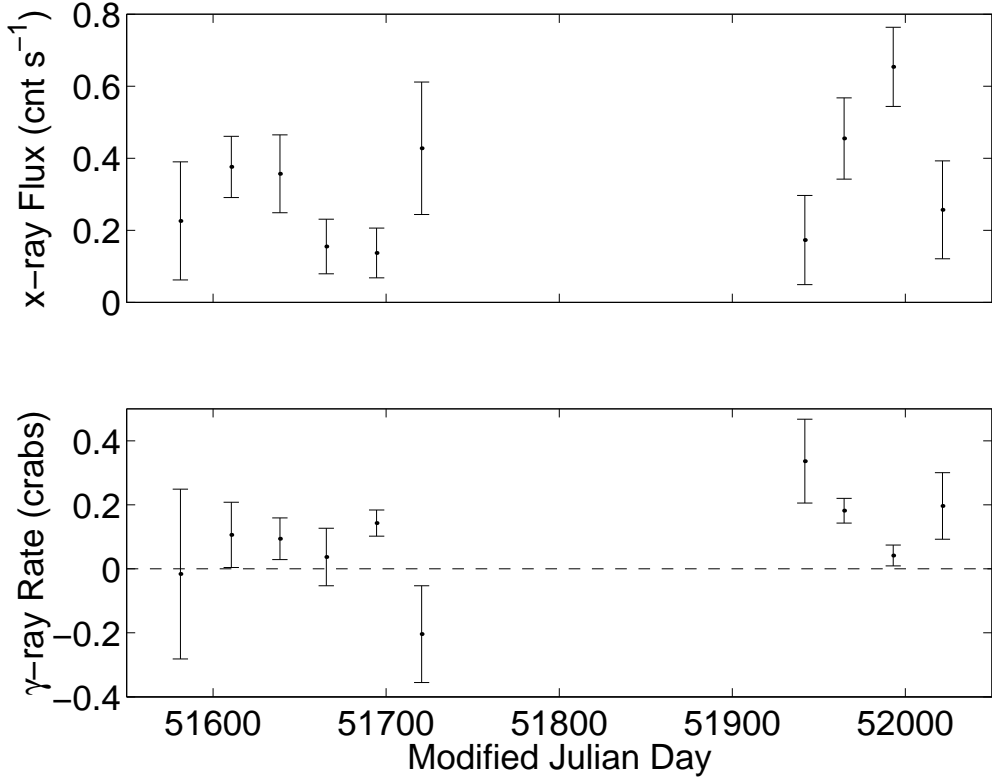


Fig. 3.— Top: The mean x-ray rate for 1H1426+428 for each month during 2000 and 2001 from the ASM on RXTE. The data are only plotted for months during which γ -ray data were also taken. Bottom: The mean γ -ray rate from 1H1426+428 for each month calculated using the alternative method for background estimation. This rate is plotted in units of the γ -ray rate from the Crab for that year. The detected Crab rate was $2.45 \gamma \text{ min}^{-1}$ during 2000 and $3.36 \gamma \text{ min}^{-1}$ during 2001.

6. Spectral Characteristics of 1H1426+428

The TeV flux from 1H1426+428 is weak and near the threshold of sensitivity of the 10m γ -ray telescope. The photon flux is so small that it is impractical to apply standard spectral analysis techniques, for example, Mohanty et al. (1998), to these data. In fact, only the differential flux from the source for the energy at which the telescope is most efficient at detecting γ -rays, can be evaluated with reasonable accuracy. Such a flux estimate accounts mostly for the photons with energies corresponding to the peak in the differential detection rate of the telescope. This energy, E_p , depends on the spectral index of the source in question. For observations of 1H1426+428 with the Whipple telescope in 2001, E_p was found to be between 280 - 360 GeV. The rate of change of the number of excess events, presumably photons from the source, with the total amount of light in the Čerenkov image, the *size*, is directly related to the spectral index of the source. This relationship is established using Monte Carlo simulations; the spectral index of the source in the vicinity of E_p is then evaluated. This in turn allows estimates of E_p for this spectral index, and the differential and integral fluxes to be improved by reducing the uncertainty due to the unknown spectral index.

Figure 4 shows the excess events detected from the direction of 1H1426+428 as a function of integrated Čerenkov light in the shower image. For comparison, this plot also shows the excess events detected from the Crab Nebula after a 4.1 hour exposure, which was chosen to produce a similar maximal excess of $\sim 10^3$ events as was found during the 32.5 hours of observation of 1H1426+428 during 2001. The lowest *size* cut of 366 digital counts is the result of signal to noise optimization of the 1H1426+428 data, producing an overall significance close to $+6\sigma$. The highest *size* cut, 840 digital counts, is limited by the rapidly declining significance to the level of $+3.5\sigma$. To a first approximation, the dependence of the excess events on the logarithm of the *size* cut applied, is a linear function whose slope is monotonically related to the spectral index of the source. This plot indicates that the 1H1426+428 spectrum is softer than the well-studied spectrum of the Crab Nebula.

Monte Carlo simulations were used to relate the observed parameters of linear fits to the data in Figure 4, to the spectral characteristics of 1H1426+428, and the Crab Nebula. The statistical correlation of the errors shown in this integral plot of excess events has been taken into account to derive optimal estimates of the spectral indices, differential and integral fluxes, and their errors. A summary of the results is given in Table 5. For the Crab Nebula a spectral index of 2.75 with an uncertainty of 6% (1σ) was derived. The peak of the differential detection rate of the Whipple telescope from a source with such a spectral index has been found to be around 360 GeV (2001 observing season). Based on the small Crab Nebula data-set, the spectral index as well as the differential and integral fluxes have been derived,

and are found to be consistent, at the 2σ level, with our previous observations (Hillas et al. 1998). Analysis of the 1H1426+428 data-set indicates a substantially steeper spectral index of 3.55 with a 13% relative error. For this spectral index and the 366 digital counts *size* cut applied in the data analysis, the differential photon detection rate peaks at ~ 280 GeV. Table 5 shows estimates of the fluxes at 390 GeV assuming the same spectral index. This energy was chosen by increasing the *size* cut until the signal to noise ratio decreased to $\sim 4.5 \sigma$; below this value the signal was not considered strong enough for reliable calculation of the 1H1426+428 flux.

Table 5. Results of the spectral analysis of 1H1426+428 and Crab Nebula data-sets.

Parameter	Crab	1H1426+428	1H1426+428
χ^2	20.60	22.72	22.72
d.f.	16	16	16
T (s)	14.7×10^3	117.3×10^3	117.3×10^3
α	2.75	3.55	3.55
E_p (GeV)	360	280	390
F_p ($\text{cm}^{-2} \text{s}^{-1}$)	1.10×10^{-10}	2.04×10^{-11}	8.76×10^{-12}
dF_p ($\text{cm}^{-2} \text{s}^{-1} \text{TeV}^{-1}$)	5.34×10^{-10}	1.86×10^{-10}	5.73×10^{-11}
νF_ν (erg $\text{cm}^{-2} \text{s}^{-1}$)	1.11×10^{-10}	2.33×10^{-11}	1.39×10^{-11}
$\frac{\Delta\alpha}{\alpha}$	0.06	0.13	0.13
$\frac{\Delta F_p}{F_p}$	0.07	0.17	0.23
$\frac{\Delta dF_p}{dF_p}$	0.11	0.25	0.17

Note. — α is the spectral index of the differential flux. E_p denotes the energy at which the differential detection rate of photons from a given source, with given observation and data analysis conditions, peaks. F_p and dF_p are estimates of the integral and differential fluxes at E_p .

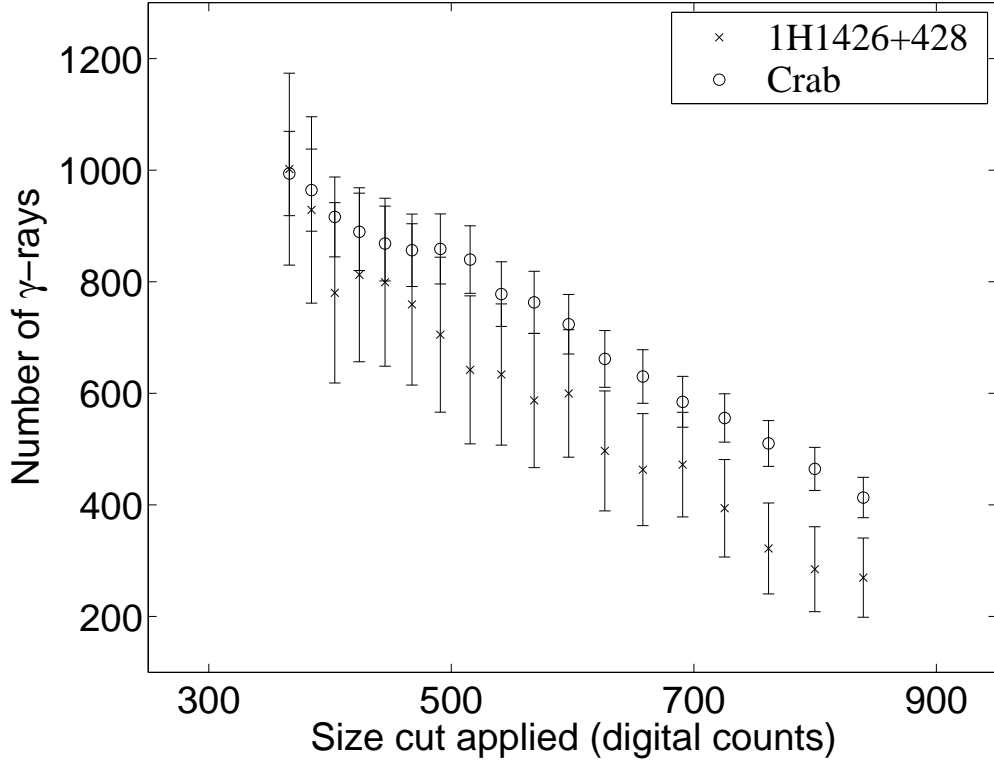


Fig. 4.— Integral excess events observed by the Whipple telescope from the directions of 1H1426+428 (crosses) and the Crab Nebula (open circles) during 2001 as a function of integrated Čerenkov light in the shower image. Exposure on the Crab Nebula was adjusted to match the total excess of 1H1426+428 at the lowest *size cut* applied, 366 digital counts. One photoelectron corresponds to ~ 3.6 digital counts.

The observed energy fluxes of 1H1426+428 at 280 and 390 GeV are shown in Figure 5 together with the predicted SED for this source suggested by Costamante et al. (2001). This figure also shows the tentative detection ($+3.1\sigma$) made by the Whipple 10m telescope during 2000. Operating at a substantially higher peak response energy at that time, the Whipple telescope observed this source at $E_{peak} \sim 430$ GeV. Based on these data an estimate of the energy flux of $0.86 \pm 0.33 \times 10^{-11}$ erg cm $^{-2}$ s $^{-1}$ has been derived. Due to the very weak signal however, we have not attempted to find the spectral index of 1H1426+428 for this data-set. As a result, the indicated error is only statistical and it does not include errors associated with the unknown spectral properties of the source. The 430 GeV peak energy itself is subject to a similar uncertainty.

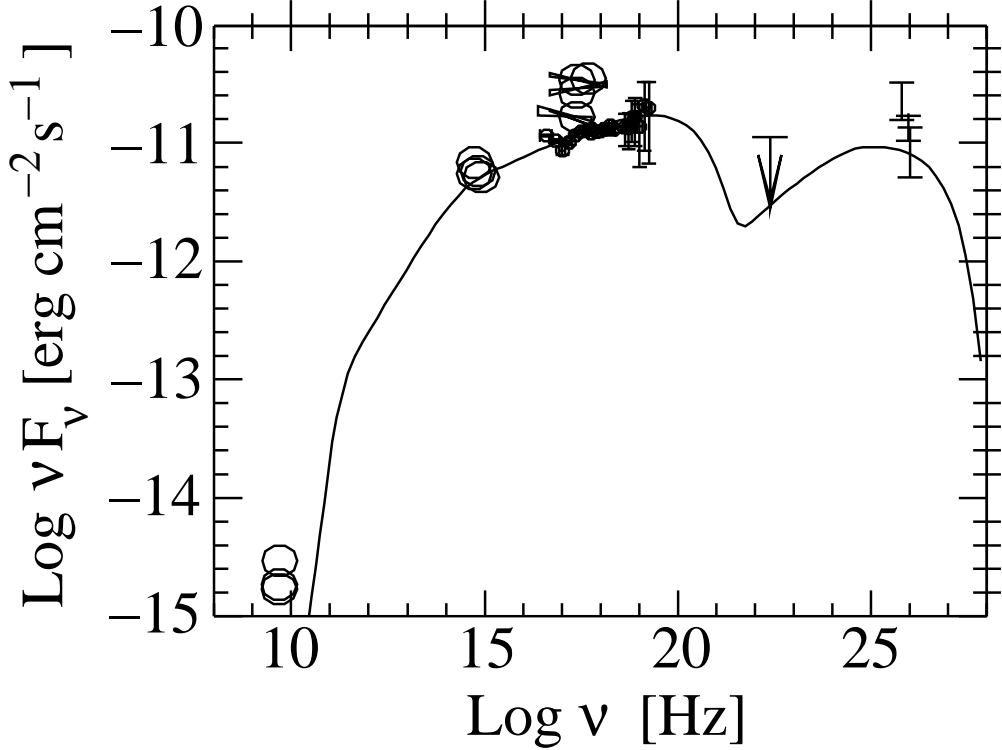


Fig. 5.— SED of 1H1426+428 from Costamante et al. (2001), along with the observational results obtained with the Whipple telescope. The 280 GeV ($\log \nu = 25.83$) and 390 GeV ($\log \nu = 25.97$) data points, derived from 2001 data-set, suggest a differential spectral index of the energy flux equal to -3.55. The 430 GeV ($\log \nu = 25.99$) point is a detection by the Whipple telescope during 2000. This result is subject to a large uncertainty associated with the weak detection and unknown spectral properties of the source. The EGRET upper limit above 100 MeV of $0.7 \times 10^{-7} \text{ cm}^{-2} \text{ s}^{-1}$ is also shown as are the fluxes from various x-ray, optical, and radio experiments, all taken from Costamante et al. (2001).

7. Discussion

Observations of 1H1426+428 with the Whipple 10m telescope since 1995 have returned consistently positive excesses although the statistical significance has not always been high. 1H1426+428 was on the very short list of predicted TeV emitters published by the *BeppoSAX* collaboration (Costamante et al. 2000a) and was also singled out as the most probable TeV emitter amongst these due to the high frequency of its synchrotron peak. It was observed as part of a BL Lac survey at the Whipple Observatory between 1995 and 1998, and was singled out for more extensive observations between 1999 and 2001. The strongest evidence for VHE emission was recorded during the 2000 and 2001 observing seasons, with signals at the 3.1σ and 5.5σ levels, respectively, being detected. Although it is difficult to combine results from different configurations of the camera, the combined significance of the results from 2000 and 2001 is clearly equivalent to a greater than 5σ detection, the usual level required to establish the existence of a new TeV source.

There have been two occasions (in 1999 and in 2000) when there was marginal evidence for a transient signal from 1H1426+428. In 1999, after 2.3 hours of observations (over two nights) a signal at the $+3.1\sigma$ level was recorded while in 2000, a signal at the $+3.7\sigma$ level was recorded after 2.2 hours of observations (on a single night).

After 18.1 hours of observations on 1H1426+428, the CAT collaboration reported a 3σ upper limit of $3.54 \times 10^{-11} \text{ cm}^{-2} \text{ s}^{-1}$ at an energy threshold of 250 GeV (Piron 2000). These observations were carried out at the beginning of February 1999 in response to an announcement from the *BeppoSAX* and the RXTE/ASM teams, which revealed 1H1426+428 to be transitioning to a high state.

If independently verified, the observations reported here represent an important addition to the catalog of TeV-emitting BL Lacs (Table 6). That the source was predicted to be a TeV γ -ray source based on its x-ray spectrum is important in that it signifies the maturity of the observational techniques and the theoretical understanding of BL Lacs. It reinforces the symbiosis between observations at x-ray wavelengths, particularly in hard x-rays, and those at TeV energies, particularly those with good sensitivity below energies of 1 TeV. The existence of a population of sources whose most prominent emission is at energies of 10-100 keV and 300-1000 GeV points to a fruitful overlap between the next generation of ground-based atmospheric Čerenkov telescopes (Weekes et al. 2001) and the future hard x-ray experiment, EXIST (Grindlay et al. 2000). It is remarkable also in that this source, like Mrk 501 and 1E2344+514, is not included in the 3rd EGRET Catalog, supporting the interpretation of Ghisellini (1999) that in blazars sufficiently powerful to be detected readily by EGRET, the spectrum will terminate at lower energies and not extend to the TeV domain.

Table 6. Extra-galactic TeV Sources (Catanese & Weekes 1999)

Source	Type	z	Discovery	Group	EGRET
Markarian 421	HBL	0.031	1992	Whipple (Punch et al. 1992)	yes
Markarian 501	HBL	0.034	1995	Whipple (Quinn et al. 1996)	yes
1ES 2344+514	HBL	0.044	1997	Whipple (Catanese et al. 1998)	no
1ES 1959+650	HBL	0.048	1999	Telescope Array (Nishiyama et al. 2000)	no
PKS 2155-304	HBL	0.116	1999	Durham (Chadwick et al. 1999)	yes
1H1426+428	HBL	0.129	2001	Whipple (Horan et al. 2000, 2001a, 2001b)	no
3C66A	LBL	0.444	1998	Crimea (Neshpor et al. 1998)	yes
BL Lacertae	LBL	0.069	2001	Crimea (Neshpor et al. 2001)	yes

Although the properties of 1H1426+428 reported here are scanty in comparison with the other, better studied TeV BL Lacs, they agree in principle with the characteristics now well established for Mrk 421 and Mrk 501 (and to a lesser extent, 1ES 2344+514). Although the flux from 1H1426+428 is low, there is some evidence for time variability. There is also an indication of a hard γ -ray spectrum. There is no evidence for a correlation of x-ray and TeV γ -ray fluxes (unlike Mrk 501) but the sensitivity of observations to date is limited and even in the stronger sources this correlation has been shown to be complicated.

Ghisellini (1999) has proposed that there is a continuous sequence of BL Lacs with the peak of the synchrotron spectrum increasing as the luminosity decreases. 1H1426+428 is another example of an "extreme" BL Lac characterized by a synchrotron spectrum that may peak near 100 keV and a relatively weak luminosity. These objects are the best candidates for TeV emission based on Compton-synchrotron models of BL Lac jets. However, the observed variations in sources such as Mrk 501 cannot be accounted for by simple one-zone homogeneous self-Compton models and may require another source of optical target photons. It will require the detection of a greater population of sources such as 1H1426+428 to test these models fully. It has been noted (Ghisellini 1998) that these TeV-emitting BL Lacs are also characterized by a relatively strong radio luminosity and that the radio luminosity may be a measure of the density of additional seed photons at infrared-optical wavelengths needed to explain the TeV emission.

This is the most distant of the TeV-detected BL Lacs classified as HBL, and hence it has promising implications for the detection of more BL Lacs at $z > 0.1$. Stronger detections of such sources, which allow an accurate measure of the TeV energy spectrum, may place significant limits on the density of the intergalactic background light. The steep spectrum derived here is consistent with many models of intergalactic absorption but could also be intrinsic to the source.

Interpretation of the theoretical prediction of the intrinsic spectrum of 1H1426+428 and the observational results reported in this paper are complicated by the possible strong attenuation of the high energy photons by the diffuse intergalactic infrared background. The appearance of such a cutoff in the spectra of TeV extragalactic sources was suggested in one of the pioneering works on TeV γ -ray absorption, by Stecker, de Jager & Salamon (1992), for the quasar 3C 279 ($z = 0.54$). A later paper (V. V. Vassiliev et al., in preparation) will discuss this subject in detail in relation to 1H1426+428; here we note only that at 280 GeV the attenuation optical depth can be anywhere between z of 0.1 and 1.0 depending on the extreme upper and lower limits known for the density of the extragalactic background light. Due to this potentially large absorption effect it is possible, for example, that the intrinsic spectral index of this source is softened by ~ 1.75 to produce the observed value

of 3.55, if the intrinsic properties of 1H1426+428 are similar to those of Mrk 501 (Vassiliev et al. 2001). It remains certain however, that being the most distant HBL detected at sub-TeV energies, the observed spectral properties of 1H1426+428 and the understanding of its intrinsic characteristics from multiwavelength observations will provide the most constraining data for extragalactic background light studies.

8. Acknowledgments

The authors would like to thank Kevin Harris, Joe Melnick, Emmet Roach, and all the staff at the Whipple Observatory for their support. We also thank the referee for many constructive and useful suggestions. This research was supported in part by the U. S. Department of Energy, PPARC, and Enterprise Ireland.

A. Data Log for 2000 and 2001 Observations

Table 7: Data log for the 2000 and 2001 1H1426+428 Observations

MJD Start Time [Mode]				
51577.48031 [p]	51672.28898 [t]	51941.43213 [t]	51970.44161 [t]	51994.37299 [p]
51577.52101 [t]	51687.17778 [t]	51941.52991 [t]	51970.49679 [t]	51994.41703 [p]
51578.49144 [p]	51687.19735 [t]	51942.43760 [t]	51970.51712 [t]	51995.49070 [p]
51579.47485 [p]	51687.21689 [t]	51944.49363 [t]	51971.43684 [t]	51996.43112 [t]
51579.51770 [t]	51687.23145 [t]	51957.37136 [p]	51971.45942 [t]	51996.47550 [t]
51581.48048 [p]	51688.17238 [p]	51957.39284 [t]	51972.44811 [t]	51997.35435 [p]
51585.50929 [t]	51689.17450 [p]	51959.39676 [p]	51972.47175 [t]	51997.44241 [t]
51586.50519 [t]	51690.17385 [p]	51959.42716 [t]	51986.36833 [p]	51997.46204 [t]
51604.43009 [t]	51692.20786 [t]	51959.44517 [t]	51988.33540 [p]	51998.40471 [t]
51605.40456 [p]	51692.24942 [p]	51960.37838 [p]	51988.35239 [t]	51998.44546 [p]
51607.43234 [p]	51693.16773 [p]	51960.40149 [t]	51989.38498 [t]	51999.41745 [p]
51617.42927 [p]	51694.17954 [t]	51960.44430 [p]	51989.43090 [p]	51999.45334 [p]
51632.35804 [t]	51694.19409 [t]	51960.46341 [t]	51990.39131 [t]	52000.40087 [t]
51632.37754 [t]	51694.22455 [p]	51960.48046 [t]	51990.43151 [p]	52000.44380 [p]
51635.31200 [t]	51694.26542 [p]	51960.50067 [t]	51990.46683 [t]	52020.23130 [p]
51635.33273 [t]	51694.30629 [p]	51961.37826 [p]	51991.40168 [p]	52022.57165 [p]
51636.35315 [p]	51695.17682 [p]	51961.39750 [t]	51991.41978 [t]	52046.22484 [p]
51637.30195 [p]	51695.21768 [p]	51961.43929 [p]	51991.43755 [t]	52047.31743 [t]
51638.35877 [p]	51695.25854 [p]	51961.47573 [t]	51991.46142 [t]	52049.27725 [t]
51641.30764 [p]	51696.26489 [t]	51961.49286 [t]	51991.47977 [t]	52050.19936 [p]
51642.36119 [t]	51698.17804 [t]	51962.39036 [p]	51992.38284 [p]	52050.23721 [p]
51642.37579 [t]	51699.17421 [p]	51962.40577 [t]	51992.43252 [p]	52051.19595 [p]
51644.36277 [t]	51700.23519 [p]	51962.43053 [p]	51992.47643 [t]	52051.26034 [p]
51645.36182 [p]	51701.25211 [p]	51963.38181 [t]	52275.18178 [p]	52053.23280 [p]
51659.25434 [p]	51702.28313 [t]	51963.42351 [t]	52275.18443 [t]	52055.26242 [p]
51659.29540 [t]	51702.30271 [t]	51963.46618 [t]	52275.18320 [t]	52056.30267 [p]
51667.28374 [p]	51720.18600 [t]	51963.48589 [t]	52275.18199 [t]	52071.24343 [t]
51669.26859 [p]	51721.18547 [p]	51965.45873 [t]	52275.18201 [t]	52072.21843 [t]
51672.26933 [t]	51940.53791 [t]	51967.46276 [t]	52275.18178 [t]	

Note. — The number in parentheses after the MJD gives the mode in which the data were taken: p - PAIRS, t - TRACKING.

REFERENCES

Aharonian, F., et al. 1999, A&A, 349, 11

Bradbury, S. M., Burdett, A. M., D'Vali, M., Ogden, P. A., & Rose, H. J. 1999, AIP Conf. Proc. 516, Proceedings of the 26th International Cosmic Ray Conference, ed. B. L. Dingus, D. B. Kieda & M. H. Salamon (Salt Lake City, Utah:AIP), 5, 263

Caccianiga, A., Maccacaro, T., Wolter, A., della Ceca, R., & Gioia, I. M. 1999, ApJ, 513, 51

Catanese, M., et al. 1998, ApJ, 501, 616

Catanese, M., & Weekes, T. C. 1999, PASP, 111, 1193

Cawley, M. F., Fegan, D. J., Harris, K., Kwok, P. W., & Hillas, A. M. 1990, Experimental Astronomy, 1, 173

Cawley, M. F. 1993, in Towards a Major Cherenkov Detector -II, ed. R. C. Lamb, (Calgary, Canada), 176

Chadwick, P. M., et al. 1999, ApJ, 513, 161

Costamante, L., et al. 2000a, Proceedings of X-ray Astronomy '99 - Stellar Endpoints, AGN and the Diffuse Background, (Bologna, Italy), in press (astro-ph/0001410)

Costamante, L., et al. 2000b, Proceedings of the 4th Italian Conference on AGNs (MemSAIt), in press (astro-ph/0007020)

Costamante, L., et al. 2001, A&A, 371, 512

Finley, J. P., et al. 2000, AIP Conf. Proc. 515, GeV-TeV Gamma Ray Astrophysics Workshop : Towards a Major Atmospheric Cherenkov Detector, ed. B. L. Dingus, D. B. Kieda & M. H. Salamon (Snowbird, Utah:AIP), 301

Finley, J. P., et al. 2001, Proceedings of the 27th International Cosmic Ray Conference, ed. M. Simon, E. Lorenz & M. Pohl, (Hamburg, Germany:IUPAP), 7, 2827

Fossati, G., et al. 1998, MNRAS, 299, 433

Ghisellini, G. 1998, MNRAS, 310, 451

Ghisellini, G. 1999, Astroparticle Physics, 11, 11

Giommi, P., Padovani, P., & Perlman, E. 2000, MNRAS, 317, 743

Grindlay, J., et al. 2000, AIP Conf. Proc. 510, The Fifth Compton Symposium, ed. M. L. McConnell & J. M. Ryan, (Portsmouth, New Hampshire:AIP), 784

Hartman, R. C., et al. 1999, ApJS, 123, 79

Hillas, A. M., et al. 1998, ApJ, 503, 744

Holder, J., et al. 2001, Proceedings of the 27th International Cosmic Ray Conference, ed. M. Simon, E. Lorenz & M. Pohl, (Hamburg, Germany:IUPAP), 7, 2613

Horan D., et al. 2000, HEAD Meeting, (Honolulu, Hawaii), No. 32, 05.03

Horan D., et al. 2001a, AIP Conf. Proc. 578, Gamma-Ray Astrophysics 2001, ed. S. Ritz, N. Gehrels & C. R. Shrader, (Baltimore, Maryland:AIP), 324

Horan D., et al. 2001b, Proceedings of the 27th International Cosmic Ray Conference, ed. M. Simon, E. Lorenz & M. Pohl, (Hamburg, Germany:IUPAP), 7, 2622

Kerrick, A. D., et al. 1995, ApJ, 452, 588

Krennrich, F., et al. 1999, ApJ, 511, 149

Krennrich, F., et al. 2001, ApJ, 560, L45

Laurent-Muehleisen, S. A., Kollgaard, R. I., Feigelson, E. D., Brinkmann, W., & Siebert, J. 1999, ApJ, 525, 127

Levine, A. M., et al. 1996, ApJ, 469, L33

Mukherjee, R., et al. 1997, ApJ, 490, 116

Mohanty, G., et al. 1998, Astroparticle Physics, 9, 15

Neshpor, Y. I, Stepanyan, A. A, Kalekin, O. P., Fomin, V. P, Chalenko, N. N., & Shitov, V. G. 1998, Astronomy Letters, 24, L134

Neshpor, Y. I, Chalenko, N. N, Stepanian, A. A., Kalekin, O. R, Jogolev, N. A, Fomin, V. P., & Shitov, V. G. 2001, Astronomy Reports, 45, 249

Nishiyama, T., et al. 2000, AIP Conf. Proc. 516, Proceedings of the 26th International Cosmic Ray Conference, ed. B. L. Dingus, D. B. Kieda & M. H. Salamon (Salt Lake City, Utah:AIP), 3, 370

Padovani, P., & Giommi, P. 1995, ApJ, 444, 567

Perlman, E. S., Padovani, P., Giommi, P., Sambruna, R., Jones, L. R., Tzioumis, A., & Reynolds, J. 1998, AJ, 115, 1253

Pian E., et al. 1998, ApJ, 492, L17

Piron, F., 2000, Université de Paris-Sud U. F. R. Scientifique d'Orsay, unpublished PhD Thesis

Punch, M., et al. 1992 Nature, 358, 477

Quinn, J., et al. 1996, ApJ, 456, L83

Remillard, R. A., Tuohy, I. R., Brissenden, R. J. V., Buckley, D. A. H., Schwartz, D. A., Feigelson, E. D., & Tapia, S. 1989, ApJ, 345, 140

Reynolds, P. T., et al. 1993, ApJ, 404, 206

Stecker, F. W., de Jager, O. C., & Salamon, M. H. 1992, ApJ, 390, L49

Vassiliev, V. V., et al. 2001, Proceedings of the 27th International Cosmic Ray Conference, ed. M. Simon, E. Lorenz & M. Pohl, (Hamburg, Germany:IUPAP), 7, 2725

Weekes, T.C. 2001, AIP Conf. Proc. 578, Gamma-Ray Astrophysics 2001, ed. S. Ritz, N. Gehrels & C. R. Shrader, (Baltimore, Maryland:AIP), 324

Weekes, T.C., et al. 2001, Astroparticle Physics, in press

Wood, K. S., et al. 1984, ApJS, 56, 507